Ben-Gurion University of the Negev

Faculty of Humanities and Social Sciences

Department of Geography and Environmental Development

A study of anthropogenic influence on soil development in central Israel using a soilscape evolution model

THESIS SUBMITTED IN PARTIAL FULFILLMENT OF THE REQUIREMENTS FOR THE MASTER OF ARTS DEGREE

Dori Katz

Under the supervision of:

Prof. Tal Svoray

Dr. Sagy Cohen

Dr. Oren Ackermann

March 2018

Ben-Gurion University of the Negev

Faculty of Humanities and Social Sciences

Department of Geography and Environmental Development

A study of anthropogenic influence on soil development in central Israel using a soilscape evolution model

THESIS SUBMITTED IN PARTIAL FULFILLMENT OF THE REQUIREMENTS FOR THE MASTER OF ARTS DEGREE

Dori Katz

Under the supervision of: Prof. Tal Svoray, Dr. Sagy Cohen, Dr. Oren Ackermann

Signature of student:  Date 15.3.18

Signature of supervisor: 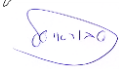 Date 15.3.18

Signature of supervisor:  Date 15.3.18

Signature of supervisor:  Date 15.3.18

Signature of chairperson

Of the committee for graduate studies:  Date 19.3.2018

March 2018

Acknowledgments

This research was a long journey that did not only teach me about soils, landscapes and everything between them, this was a journey to become a scientist. I could not achieve this great accomplishment without the dedicated guidance and support from my three outstanding supervisors. First, to Tal, who met me one late night on the summer of 2015. We talked about modeling, spatial data, human influences and how these can work together to improve our understanding on how human activity affects the soils we live on. Thank you for embracing me in to your lab, supporting my new ideas and keeping a flexible open mind for new approaches. To Sagy, thank you for the help with running and analyzing the mARM5D model which this study couldn't have done without it. Thank you for the insistence for details and the professional insights, and I want to point out that I learned a lot from your reviewing and writing. And to Oren, it was a pleasure talking to you about anything, if it was work arguments or personal advice, it was always with a friendly smile and a knock knock joke at the end. Your extensive knowledge has contributed significantly to the success of this study.

I would like to thank Dr. Michael Dorman and Oron Moshe for the dedicated technical support. Nothing was too much for you, you guys are awesome!

A major gratitude is sent to Arthur Khozin, my lab mate. Thank you for being there as a close friend, like brothers in Arms just in the academy :) . Thanks are also extended to Nitzan Swet and Din Danino for the entire PSA analysis.

One of the best things I'm taking with me is a rare person who I can now define as a very close friend, thank you Omry Avni. I am so happy that the academy brought us to meet, you are an extraordinary friend, I don't know what I have done without the ping pong table!

Thank you, dear family, for believing in me and supporting me.

Last but defiantly not least, thank you my amazing wife for pushing and supporting all the way, I could not get to where I am today without you. And to my beautiful daughter, Ayala, for teaching me every day the meaning of life, this is for you.

Table of Content

Figure List

Abstract

Anthropogenic activities were shown to have considerable influence on soil degradation throughout history worldwide. Some suggest that anthropogenic activity is responsible for the soil-depleted hillslopes observed in the "Shfela" region of central Israel.

The overarching goal of this research is to advance our understanding of the Shfela region, and its potential soilscape response to varying degrees (duration) of human disturbances. Our study site is located in the sub-humid climate zone, close to the transition to the semi-arid zone. We focused on a representative hillslope that has not been studied before. Elevation data of 1m resolution was extracted from an aerial Lidar cloud data with a density of 0.5m; soil depth and high-resolution PSD was analyzed from soil pits on the field site.

Following an extensive sensitivity analysis and calibration process, we ran the mARM5D soil-scape evolution model for 5 simulation scenarios, each scenario with a different human disturbance duration on the soil. The results of the simulation scenario analysis suggest that it is unlikely that the site ever had a considerably deep layer of soil (more than 1m). Therefore, it is hard to regard anthropogenic activity as the main factor leading to the soil-depleted hillslopes observed in this region. The results demonstrate that climate fluctuation leading to lower aeolian deposition and higher soil erosion rates could have shifted local soil evolution from a net accumulation mode (or static equilibrium), mainly based on aeolian deposition, to a soil erosion mode driven by an increase in discharge and diffusive mechanisms.

This research takes us one step closer in utilizing the mARM5D soil-scape evolution model on landscapes that were subjected to aeolian deposition in order to reconstruct the soil-landscape-climate-human interaction over history, or in the future.

1. Introduction

Anthropogenic activities were shown to had considerable influence on soil degradation throughout history worldwide (van Andel et al., 1990 (Greece); Anselmetti et al., 2007 (Guatemala); Bruckner, 1986 (Mediterranean); Butzer, 2005(Spain, Greece); Dan et al., 1972(Israel); Dietrich and Perron, 2006; Garcia-Ruiz, 2010(Spain); Kaplan et al., 2009 (Europe); Singer, 2007 (Israel); Villamil et al., 2001 (Argentina); Yaalon, 1997 (Mediterranean); Zheng, 2006 (China)). Studies have shown that most Mediterranean soilscapes (soil-landscapes) are often polygenetic, a product of aeolian deposition and *in situ* bedrock weathering processes. Both of these soil production and evolution processes can be strongly affected by climatic fluctuations and anthropogenic influences (Yaalon, 1997). Anthropogenic influences, primarily deforestation and vegetation clearance, are significant factors in Mediterranean Soil-Scape Evolution (SSE) as this region has experienced long-term (> 5000 years) human influences (Bruckner, 1986).

Deforestation and vegetation clearance accelerated throughout the ancient times (Greeks and Romans periods) and continued since at different rates (Neumann et al., 2010). This eventually caused enhanced erosion of, in some regions, well-developed soils. As a result, modern Mediterranean soilscapes are often characterized by highly soil-depleted (exposed bedrock) hillslopes and massive valley fills (Yaalon, 1997). Anthropogenic influence on soil evolution and erosion was widely studied throughout the Mediterranean (Italy, Greece, Israel, Spain, Turkey; van Andel et al., 1990; Bruckner, 1986; Inbar, 1992; Recep and Abdullah, 2015). Butzer (2005) concludes that the different points of view on anthropogenic influence converge to a general agreement that overall anthropogenic activities have led to the soil-depleted landscapes we see today throughout the Mediterranean basin. In contrast, Avni et al (2006) concluded that in the Negev highlands (southern to the "Shfela" region), natural mechanisms are responsible to local degradation of the soils on hillslopes.

Robust investigation of pedogenesis and soilscape processes and dynamics is extremely challenging due to the massive amount of data that must be collected and analyzed. Furthermore, the different processes and drivers controlling soil evolution can differ considerably in time and space making the analysis of in situ observation very difficult. Numerical models can help alleviate these challenges by providing a framework for developing and testing complex hypothesis on the interactions between pedogenesis and landscape processes and their potential response to external drivers (e.g. anthropogenic and climatic) (Cohen et al., 2014).

There are many models that simulate soil evolution and landscape evolution separately (Minasny et al., 2015). Nevertheless, based on extensive literature review, there are only three known combined SSE Models (SSEM): MILESD (Vanwalleghem et al., 2013), LORICA (Temme and Vanwalleghem, 2016) and mARM5D (Cohen et al., 2015). The main goal of these models is to improve our understanding of soil-landscape interactions by providing a framework to develop and test hypotheses focusing on the interactions within the soilscape system and its response to external drivers (Minasny et al., 2015; Temme and Vanwalleghem, 2016).

As Cohen et al (2017) widely explained, aeolian dominated soilscapes are fundamentally different from in situ bedrock-weathering dominated soilscapes. Thus, to properly investigate and explain aeolian dominated soilscapes there is a need for soilscape evolution models that consider the unique properties of aeolian dominated soilscapes. The mARM5D model (*Cohen et al.* 2014) is the only SSEM that can simulate aeolian deposition. It also been used to simulate a semi-arid field site in southern Israel (Cohen et al., 2017).

The overarching goal of this research is to advance our understanding about the "Shfela" region of central Israel, and its potential soilscape response to varying degrees (duration) of human disturbances. (Dagan, 1992, 2002, 2006) . Most of the hillslopes in this region are covered with rock outcrops (of calcrete crust known locally as Nari) with shallow soil

pockets between them. Is this phenomenon an outcome of human activity or the outcome of the natural equilibrium between soil production and erosion?

Sub-goals of the research are to investigate the feasibility that human activity is connected to the degraded hillslopes observed on the field site translated to shallow soils, and the potential effects of introducing human activities to the hillslope on the PSD of the soil surface layer.

2. Materials and Methods

2.1.Field site

The field site is a single hillslope, extending from south-east to north-west, located in the low hills of the "Shfela" region, near the settlement of Lachish in central Israel (31.604N/34.839E, Figure 1). This study site was selected due to the combination of rich anthropogenic history, shallow hillslopes and the fact that it has not been studied before.

The hills are composed of Senonian and Oligocene soft chalk (Picard et al., 1965). Most of this chalk is now covered by a hard calcareous crust (nari, calcrete) (Dan et al., 1962; Dan and Yaalon, 1966). Younger sediments that fill the valleys between the hillslopes, mainly consist of Miocene conglomerates (Sneh, 2008) and Pleistocene aeolian clayey deposits. The soils on the hillslopes cover either the crust (Brown rendzina) or the soft chalk itself (pale rendzina).

Brown Rendzina and Brown Forest soils have many similar characters and are considered two related soils. Although according to Dan et al. (1972) they all belong to the Rendzina soil group and by Rvikovitch (1969) they are classified as Brown Mediterranean Forest soil, in the current classification system used in Israel they are grouped into one classification unit (Singer, 2007). Here, we will approach these soils by the general name "Brown Rendzina".

The main characters of the Brown Rendzina are: non-calcareous to calcareous A(B)C soils, formed on nari (calcrete) lime crust, hard chalk and sporadically on hard limestone. Brown to Dark-Brown depending on organic matter and parent material, fine textured, granular structure to subangular blocky in the deeper layer and organic matter content between moderately high to high. The soil is relatively shallow (10-60 cm) and is organized in soil "pockets", thus the shift between the bedrock and soil is commonly sharp leading to abundance of rock outcrops on the hillslopes (Figure 1A) (Dan et al., 1972; Jenny, 1941). The mentioned soils evolve under sub-humid to humid Mediterranean climate, with annual rainfall of 400-900 mm and frequently cover exposures of Senonian chalk or Cenomanian marls in the hill or mountain regions. Landscapes, where rendzina soils are dominant, consist dissected hills and plateaus with a majority ranging elevation between 200-500 m. Hillslopes in these landscapes are moderate to steep with smooth contours (Singer, 2007).

The site topography is characterized as moderate convex declining from south-east to north-west, ranging from 230m to 192m AMSL (Figure 2) and is part of the Lachish Basin. Average rainfall in this location is approximately 400 mm per year and is defined as a semi humid climate. The mean annual temperature is 20.8°C, with a maximum of 27.7°C and a minimum of 13.2°C (Israel Meteorological Service, 2011). The area of the site is 0.161 km^2. The site is located on the Mediterranean climate margin, between a Mediterranean climate to the north and a semi-arid climate to the south. This region has undergone climatic changes throughout history as well as different anthropogenic influences since the agricultural revolution (Ackermann et al., 2014; Vaks et al., 2006).

Different climatic changes subjected the region to various aeolian deposition rates, these deposits are known to be significant and are the base to most of the soil materials in this region (Bruins and Yaalon, 1992).

2.2.Measured data

The digital elevation model (DEM) used in this study was obtained from an aerial LIDAR in a resolution of 0.5m aggregated to 1x1m pixel resolution. From this DEM, a D8 flow direction, Dinf (D-infinity algorithm; Tarboron, 1997) slope (mm−1) and Dinf contributing area layers were calculated using the TauDEM tool (Tarboton, 2010). A high definition particle size distribution (PSD) was derived by ANALYSETTE 22 Micro Tec Plus (Fritsch) laser diffraction and was averaged for the hillslope based on 21 topsoil samples. Mean soil depth was driven from 43, soil to bedrock, pits.

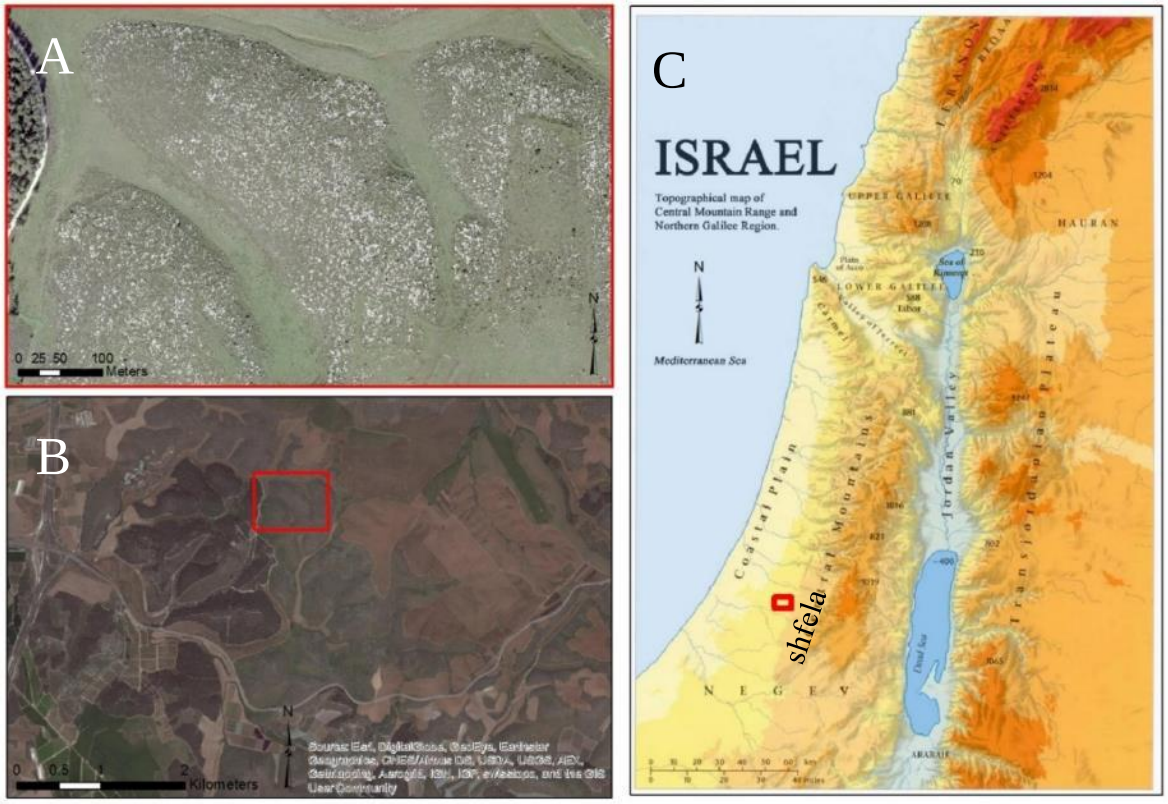

Figure 1: A- **0.25 m resolution ortophoto of the study site**; B – **ortophoto of the watershed**; C - **physical map of Israel** (Israel Science and Technology Directory, 2018)

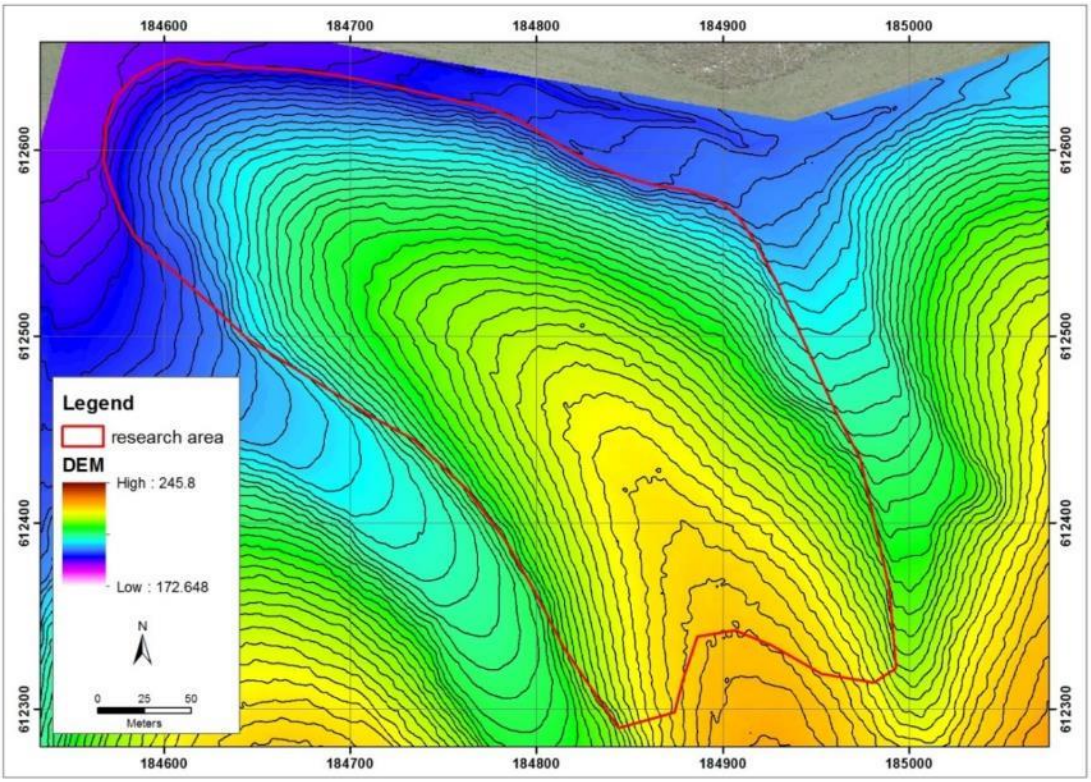

Figure 2: A Digital Elevation Model of the study site based on a 0.5m LiDAR point cloud

2.3. Modeling

2.3.1. Model Operation

The mARM5D is a modular and computationally efficient dynamic soil evolution model that simulates five soilscape dimensions, three spatial dimensions, a temporal dimension and a particle size dimension. The origin of the model is the ARMOUR model [*Willgoose and Sharmeen* 2006] that was developed into the mARM, followed by the mARM3D (Cohen et al., 2009, 2010) and recently into the mARM5D model (Cohen et al., 2015, 2017). This model contains a unique modeling approach where the soil profile is described as a vector of vectors for each grid cell. Furthermore, the PSD is also described as a vector for each layer in each grid cell, this vector quantifies the relative input of every single particle size fraction per unit mass. This exclusive method distinguishes most of the main model equations from the typical flux equations by controlling the relative change in PSD vector for each profile layer in each grid cell (Cohen et al., 2015).

The model quantifies four main processes (Figure 3):

(1) physical weathering of bedrock and regolith, assuming a mass balance break-in-two mechanism;

(2) Aeolian deposition assuming spatially uniformed annual rate of deposition.

(3) Fluvial transport, based on selective removal and transporting of particles;

(4) Diffusive transport, based on depth dependent soil creep mechanism.

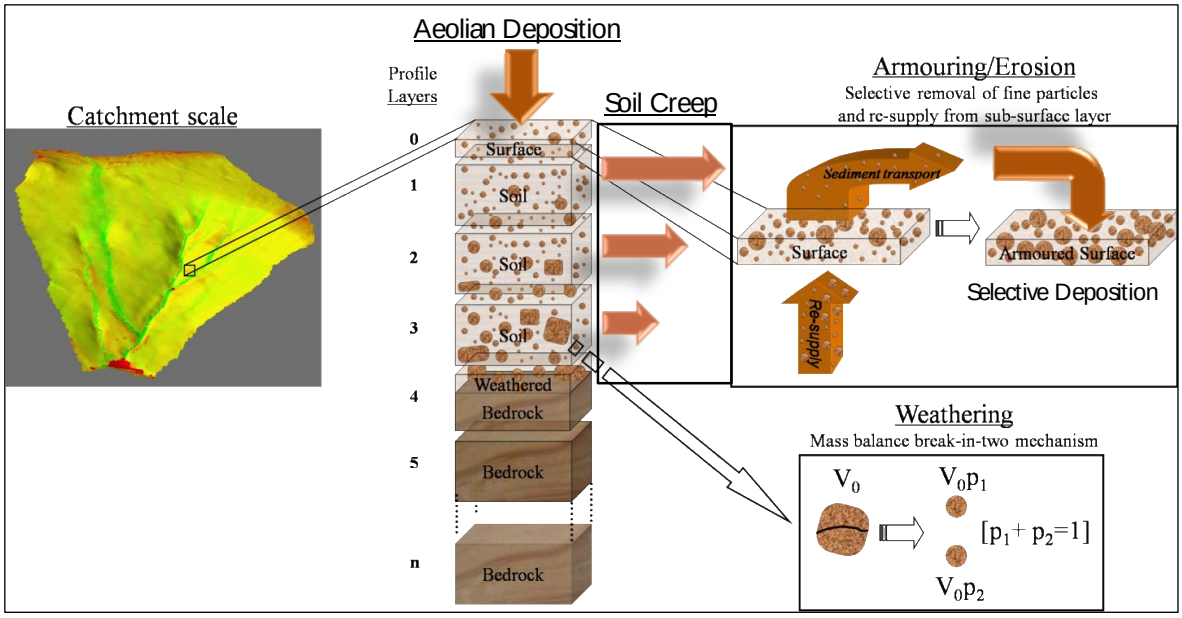

Figure 3: mARM5D model mechanisms

2.3.2. Model assumptions

Although Soil evolution combines multiple processes that include complex physical, biological and chemical processes, *Cohen et al.*, [2014, 2017] chose to include only a few of the soil evolution dynamics. This was to simplify the ultra-complex medium of the soil, allowing gaining better understanding of the model's components. The main assumptions imbedded in the model can be summarized as:

(1) Aeolian sediment is assumed to originate from outside the system, and no Aeolian erosion is considered within the simulated domain.

(2) Soil hydrology is not directly simulated.

(3) No chemical properties are simulated e.g. formation of aggregates.

(4) Entrainment is based on the particle diameter.

(5) Diffusive transport process is not particle size selective.

(6) Chemical and biological weathering processes and agents are not simulated.

2.3.3. Parameters and their calibration

Due to its complexity, the mARM5D model has a wide range of parameters, coefficients and constants (Cohen et al., 2009, 2010, 2015, 2017). All of the hard coded constants were based on Cohen et al. (2017). An extensive sensitivity analysis and calibration processes were conducted for the parameters that can be changed outside the code: (1) Discharge [Q] (2) Aeolian deposition rate (3) Soil Creep Rate [D] (4) Erodibility value [K]. The number of iterations per model run (equivalent to number of years the model run simulates) was set to 20,000 iterations (years). This number is based on the fact that the rock outcrops, which are composed of nari (calcrete) and the bedrock, composed of fractions of nari and chalk, were exposed approximately 20,000 years ago (Wieder et al., 1993).

Max soil depth was set to 200 cm to ensure sufficient depth for the model simulation. Based on 43 soil pits, soil depth in the field site ranges from 5cm up to 60cm with an average value of 25.9cm.

The bedrock of the hillslope is combined by chalk and calcrete (similar to limestone characteristics), these materials usually produce very low amounts of soil due to their solubility properties. Based on Cohen et al. (2017), bedrock weathering was set at a very slow rate of 0.01 mm/yr and was found to be negligible in comparison to the contribution of aeolian deposition.

2.3.4. Sensitivity analysis

Realistic calibration of the model parameters using field observations is not feasible for this study site due to the lack of long-term observational data for the relevant parameters and the fact that the region has undergone considerable changes in surface cover and climate over the period of interest. An extensive sensibility analysis was conducted in order to (1) elucidate the co-dependence and importance of key model parameters, and (2) select the parameter space that best match observed soil depth distribution.

Initially, aeolian deposition was accumulated in values ranging between 0.006 to 0.2 cm/y at intervals of 0.01 cm/y. As a result of defining all of the soil transportation parameters to 0, soil depth was a linear result of the aeolian deposition rate. If so, any aeolian deposition value that was higher than 0.01 cm/y exceeded the maximum soil thickness of 2 meters that is defined for this study. This was done to verify and demonstrate the soil accumulation mechanism. Finally, Aeolian deposition rate was based on the sensibility analysis and on Bruins and Yaalon (1992) and set to 0.1 mm yr^{-1}.

The sensitivity analysis, focused on three model parameters: Q – Discharge [m^3/iter], K - Erodibility value, and D - Soil Creep Rate [cm/y]. The initial parameter space was based on Cohen et al. (2017) with consideration that our site is under slight wetter conditions. Q values were simulated at a range of 0.001-0.1 at intervals of 0.001, K in the range of 0.0001-0.001 at intervals of 0.0001 and D in the range of 0.6 – 2 at intervals of 0.2. All of the sensitivity analysis simulation assumed no climate fluctuation.

2.4.Simulation scenarios

Given that the dynamics of the intensity of human activity in this region is not fully known and its direct influence on soilscape processes is challenging to asses, differences in the duration of anthropogenic activities on the landscape is simulated and analyzed in this study

The effects of climatic fluctuation on soilscape evolution in this region are relatively well established and were shown to be significant (Avni et al., 2006; Cohen et al., 2017). Climate-related fluctuations in the model parameters were similar for all five simulation scenarios and are based on the following assumptions outlined by Cohen et al. (2017):

1. Vegetation cover increase during wetter climate, reducing soil erosivity and runoff potential (Avni et al., 2006; Goodfriend, 1987; Zilberman, 1992).
2. Colluvial processes intensify during wetter climate, translated to higher diffusive sediment transport rate (Goodfriend, 1987; Zilberman, 1992).
3. Aeolian deposition rates are higher during wetter climate (Bowman et al., 1986).

Climatic fluctuations were simplified into three climate periods with different parameters magnitude for each period (Figure 4). The division was based on Vaks et al. (2006), similar to the division in Cohen et al. (2017):

1. P1: 20-12kys BP, end of the late Pleistocene. Wetter climate, increased diffusive sediment transport (scale of 1.6 relative to nowadays rate). Scale of 0.2 for erodibility and runoff rates and a scale of 1.5 for aeolian deposition.
2. P2: 12-8kys BP, early Holocene, a period of dryer climate compared to the late Pleistocene. Scale of 1.2 for diffusive rate, scale of 0.4 for erodibility and runoff, and a scale of 0.5 for aeolian deposition.
3. P3: 8-0kys BP, late Holocene, driest climate. Increased (relative to P2) erodibility and runoff to a factor 0.8, decreased diffusive rate to 0.8 and a decreased factor =of 0.2 for aeolian deposition.

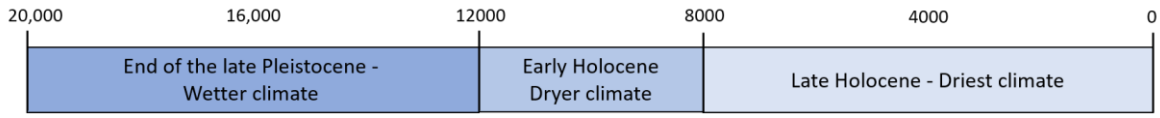

Figure 4: Timeline (BP) of the climate fluctuation in the simulated scenarios

The impact of anthropogenic activity on soil evolution in this region is manly by vegetation clearance (grazing, slash and burn), as it has direct influence on increasing runoff and erodibility of the soil surface. As mentioned, differences in the duration of anthropogenic activities on the landscape is simulated and analyzed in this study. This will help us to better understand the anthropogenic impact on the soil as a result of different durations of human interference. Based on historical evidence (Dagan, 1992, 2002, 2006; Me'ir, 2012; Uziel and Maeir, 2005) five simulation scenarios were developed. The scenarios differ in the starting time (and thus duration) of significant anthropogenic influence on the landscape.

Mohammad and Adam (2010) conducted a study on a site approximately 10 km east from our site, and found that soil cleared from vegetation results in about double the amount of soil erosion in comparison to a neighbor plot with forest cover. This led us to simulate Human impact by doubling the parameter values of K and Q in comparison to the base simulation (S0) e.g. if the K value is set on 0.0002, in human influenced times it will increase to 0.0004. This means that anthropogenic disturbance only impact fluvial sediment transport in this analysis while Aeolian deposition, rock weathering and diffusive transport is assumed to be unaffected. The above described climatic fluctuation scenario is used in all five simulation scenarios.

The five scenarios are (Figure 5):

S0: Baseline - no human activity.

S1: The Ottoman period - characterized by intense human activity in the region, started 400 years BP (Dagan, 1992, 2002, 2006; Me'ir, 2012; Uziel and Maeir, 2005).

S2: The Byzantine period - considered as the peak of human activity in the region during ancient times, started 1600 years BP (Dagan, 1992, 2002, 2006; Me'ir, 2012; Uziel and Maeir, 2005).

S3: The Iron age - started 3000 years BP (Dagan, 1992, 2002, 2006; Me'ir, 2012; Uziel and Maeir, 2005).

S4: The Agricultural Revolution - started 11000 BP (Zohary et al., 2012)

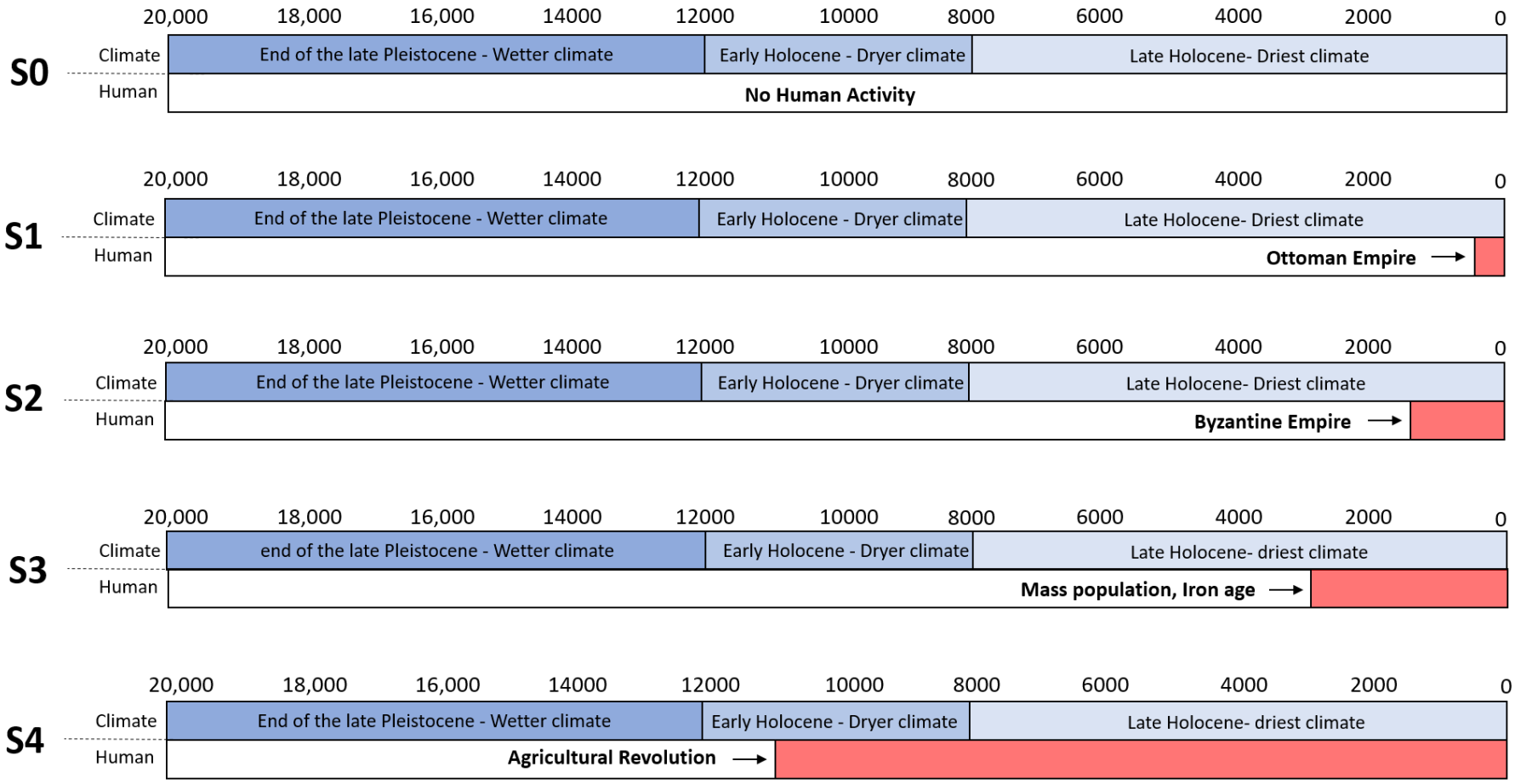

Figure 5: Discription of climate fluctuation and the initializing of human influence on a timeline (BP), on the soil, as represented in the model's parameters.

3. Results

3.1. Model calibration and sensitivity analysis

More than one thousand simulations in different parameter combination were executed. The first 200 were used to define the aeolian deposition rate and evaluating the simulation outcome with different Discharge (Q) and erodibility (K) values, while defining soil creep rate (D) to 0. Followed this, we ran 800 simulations with a defined parameter space and a systematic parameter change including the three parameters of interest (Q, K, D). Figure 6 shows the final (end of simulation) average soil depth, for each combination of the three subjected parameters (K, Q and D). The x-axis of each panel represents the Q (discharge) value for each simulation, the y-axis represents the k (erodibility) value, and each panel represent a different D (soil creep rate) value (at the title of each panel).

The decline in soil depth along x-axis (k values) is symmetrical to that in y-axis (q values), and exponential along the XY diagonal. The average soil depth value decrease with a negative correlation to d (soil-creep rate) values. While k value increases with constant intervals, the soil depth decreases in a higher power, similar with variations in q values.

Figure 7 shows the same data (average soil depth) equivalent to Figure 6, but in a different structure. The panels are divided by the parameter q, from lowest value (0.01) on the upper left to the highest on the lower right. X axis for each matrix are d values, and Y axis for each matrix are k values. The maximum and minimum values are the same as above with a remarkable difference in the relation between k influence on the average soil depth and d values. Closer isolines indicate grater change over a smaller distance, thus, d values have a consistent grater power on the final average soil depth for each of the q values. This power declines as the q values rise from 0.01 to 0.1.

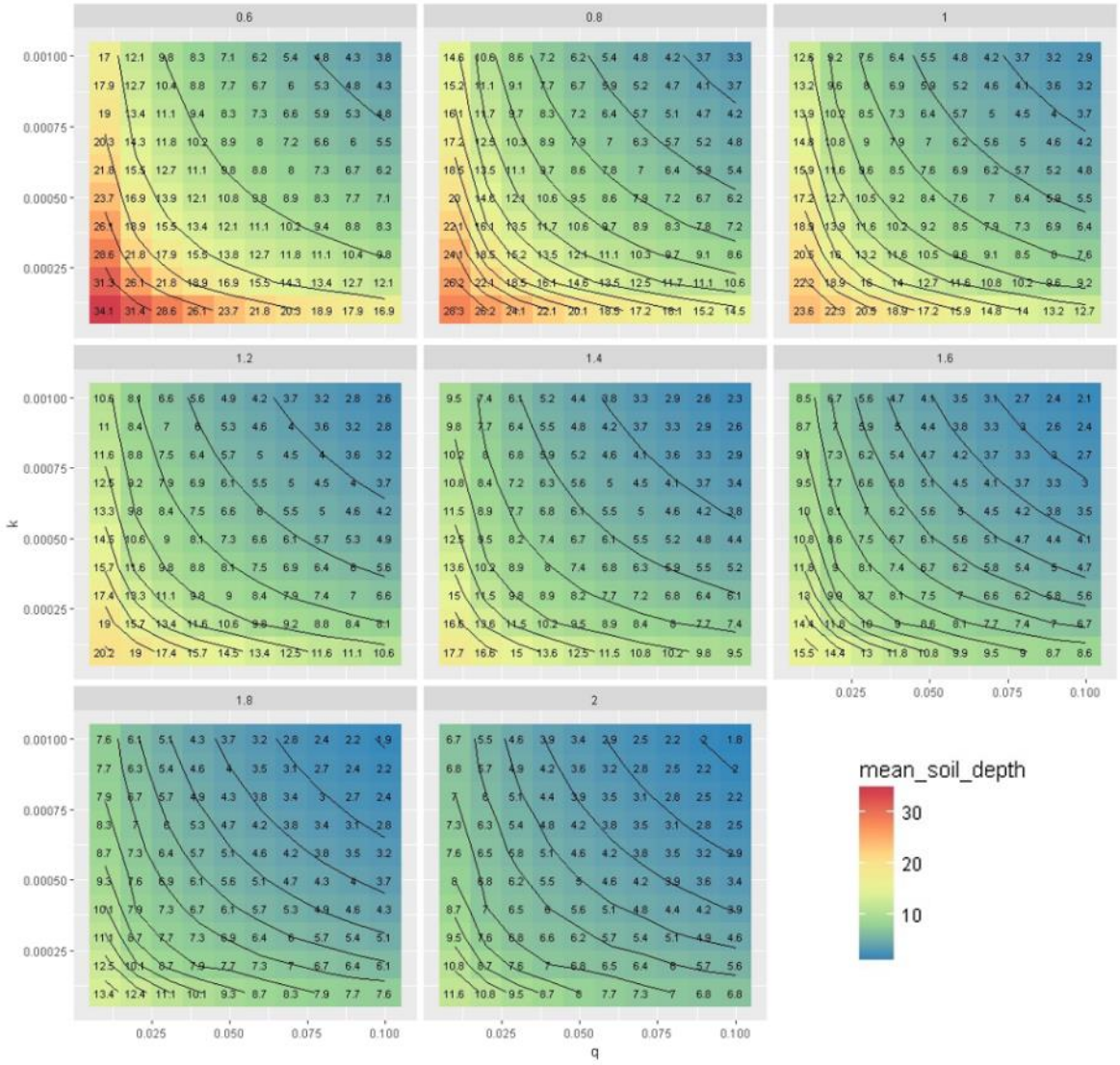

Figure 6: Average soil depth values on the hillslope. X axis in each frame are Discharge values (q), Y axis in each frame are Erodibility values (k) and the title of each frame is its Diffusive value (d). blue color represents values of 0cm and red color represents values of 34cm.

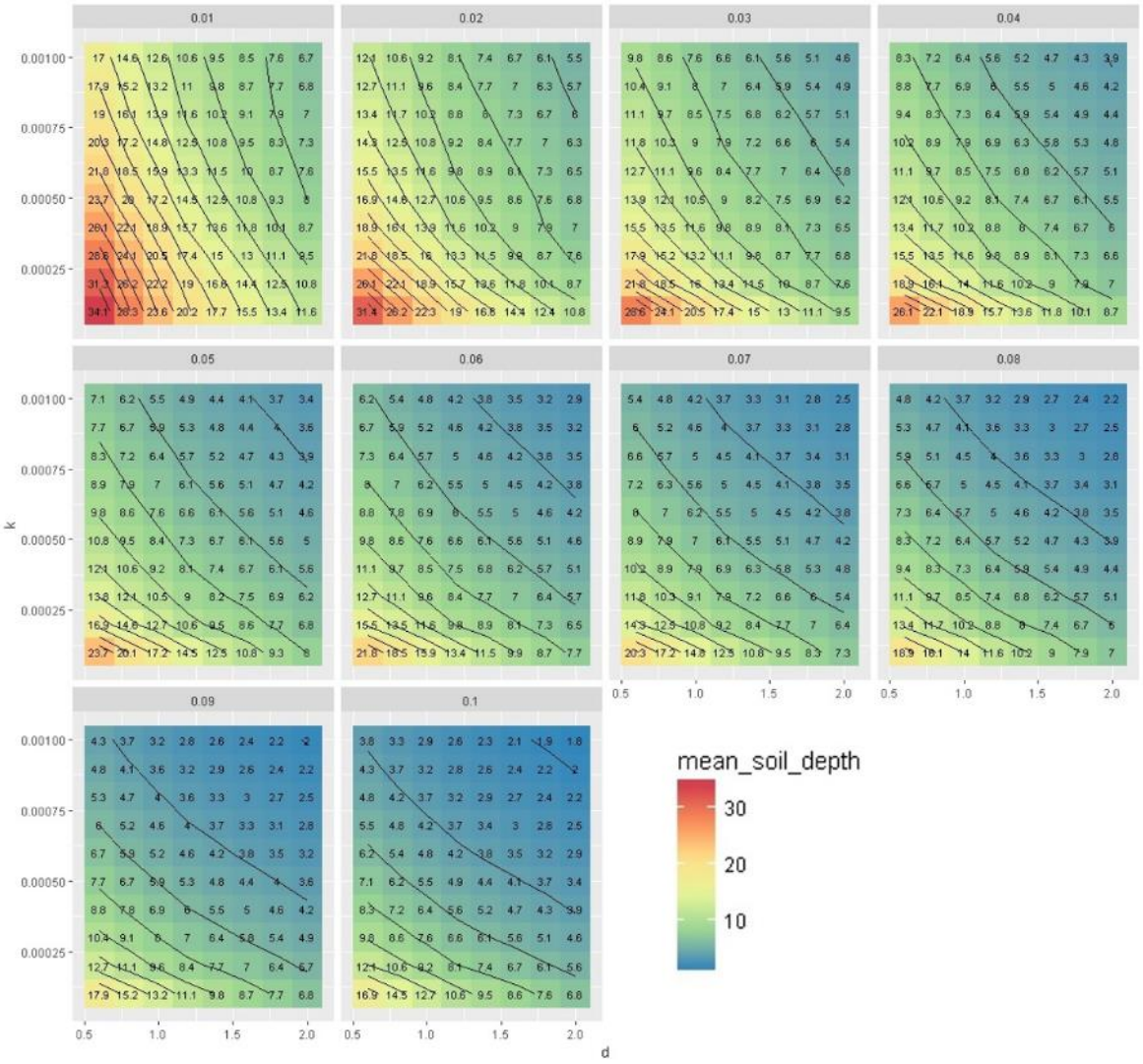

Figure 7: average soil depth values on the hillslope. X axis in each frame are Diffusive values (d), Y axis in each frame are Erodibility values (k) and the title of each frame is its Discharge value (q). blue color represents values of 0cm and red color represents values of 34cm.

Figure 8 shows again the same data as the images above (average soil depth), yet the panels are divided by the k parameter, from lowest value (0.0001) on the upper left to the highest (0.001) on the lower right. The x-axis for each panel are the d values, and the y-axis for each panel are the q values. As mentioned before, k parameter and q parameter are in the same model equation with a link of product between the two parameters. This explains the resemblance between the outcomes of different axis definitions, k values as Y axis or q values of Y axis create the same visuals.

The soil depth results of the calibration process are contained in a repeated pattern of values between 34-1.8 cm. As assumed, there is a direct correlation between low values of

the parameters and high values of soil depth. The trends are diagonal from the left lower corner of each template (deep soil, low parameter values) to the upper right corner (shallow soil, high parameter values). the rate of change is not linear and is higher in the smaller parameter values, thus suggesting that in smaller values changes affect the soil with more power.

The maximum average soil depth that the model predicted, based on values of Q=0.01, K=0.0001 and D=0.6, is 34.1 cm. The minimum average soil depth predicted, based on values of Q=0.1, K=0.001 and D=2, is 1.8 cm. A D value of 0.6 yielded the largest range of average soil depths.

The parameter values chosen to be implemented in the simulation scenarios were defined by a comparison of the average soil depth values to those that were measured at the site. Based on this assumption the closest value to 25.9 (average soil depth as measured from 43 pits) was 26.2, from the parameter combination of D = 0.6, K=0.0002, Q = 0.02.

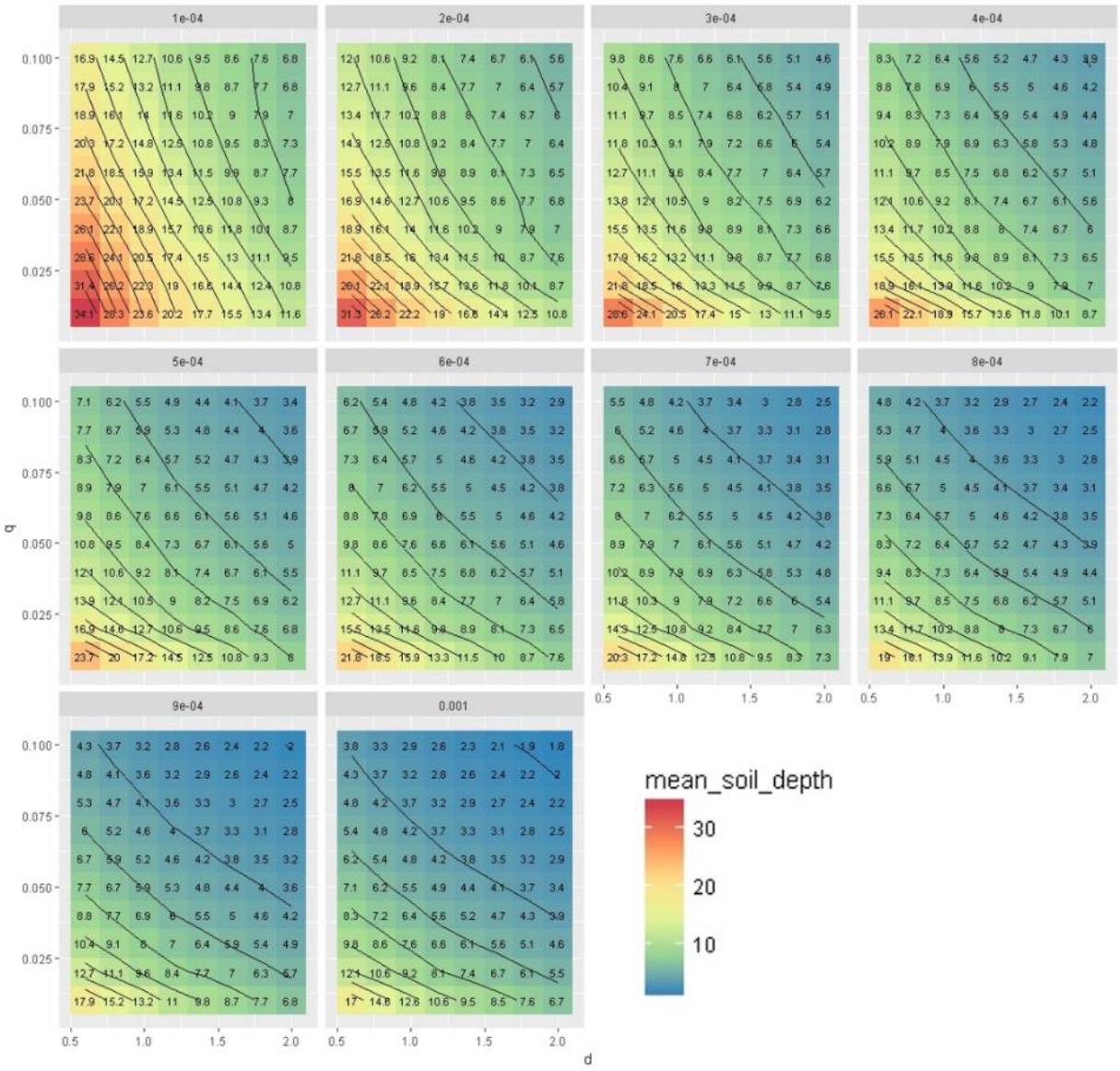

Figure 8: Average soil depth values on the hillslope. X axis in each frame are Diffusive values (d), Y axis in each frame are Discharge values (q) and the title of each frame is it's Erodibility value (k). blue color represents values of 0cm and red color represents values of 34cm.

3.2. Simulation scenarios

Human influence impacts on soilscape evolution is first investigated by comparing the relative change of average soil depth on the hillslope for each anthropogenic impact scenario (S1-S5) to the baseline scenario (S0). The Ottoman period simulation (S1), shows the least difference from the base simulation, with only a 2% lower average soil depth at the end of the simulation (Figure 9). Agriculture revolution (S5) has the highest final rate change of -22% change in average soil depth at the end of the simulation, relative to the base simulation.

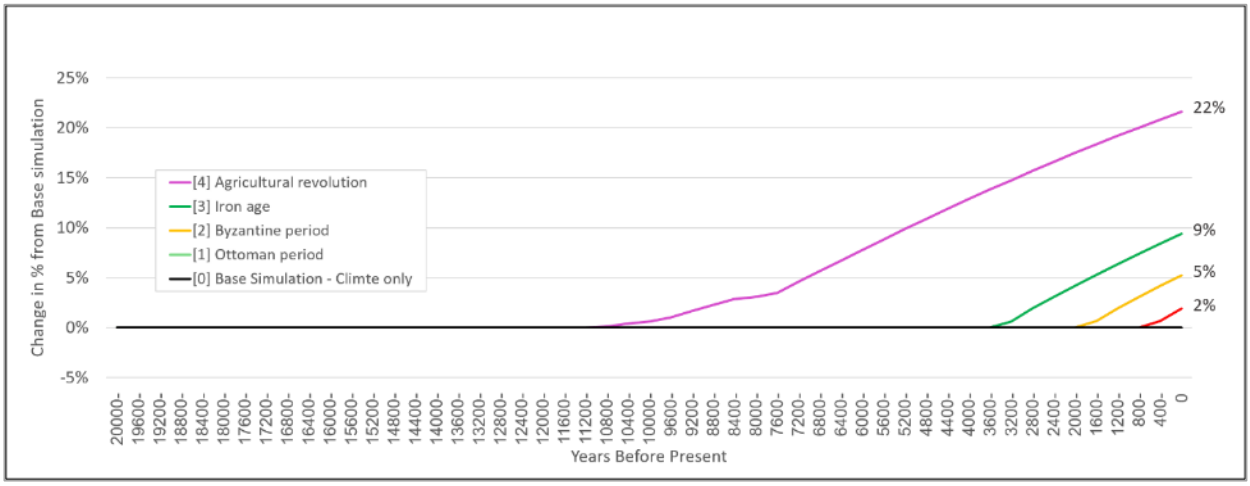

Figure 9: Change in average soil depth, realtive to the base simulation of climate fluctuation with no human impact (values in %).

For the baseline simulation (S0), there is a constant increase in the average soil depth on the hillslope, for the first 8 kyr (Figure 10), linked to a wetter climate with higher aeolian deposition rates and lower soil erosion rates. At the first 3 kyr of the simulation there is a mean addition of 5.3 (cm/kyr), this soil accumulation rate decreases for the next 5k years of the simulation (17,000-12,000 BP) and has a mean addition of 2.3 (cm/kyr), reaching a maximum average soil depth of 27.5 cm. After 8k years of simulation, dated 12,000 BP, there is a shift from positive to negative gradient in average soil depth. This is due to the simulated climate fluctuation and is characterized with a dryer climate with less aeolian deposition, higher diffusive rate and lower erodibility and runoff rates. Between 12,000 – 0

yr BP, there is somewhat steady decrease in soil depth with a mean degradation rate of 0.75 (cm/kyr). The shift from a trend of soil accumulation to soil loss occurs prior to the introduction of any human influence and is an effect of the changes in climate conditions. The baseline simulation ends with an average soil depth of 18.5 cm.

Ottoman simulation scenario (S1), introducing anthropogenic disturbance for the last 400 years of the simulation, shows increase of the soil loss rate for the last 400 years from 0.75 cm/kyr (Base Simulation) to a rate of 1 cm/kyr (Figure 10). This simulation ends with an average soil depth of 18.2 cm. The Byzantine simulation scenario (S2), introducing anthropogenic disturbance for the last 1600 years of the simulation, shows increase of the soil loss rate for the last 1600 years of the model from 0.6 cm/kyr (Base Simulation) to a rate of 0.9 cm/kyr. The simulation ends with an average soil depth of 17.6 cm. The Iron age simulation (S3), introducing anthropogenic disturbance for the last 3000 years of the simulation, shows increase of the soil loss rate for the last 3000 years of the model from 0.6 cm/kyr (Base Simulation) to a rate of 1 cm/kyr. This simulation ends with an average soil depth of 16.8 cm. The Agricultural revolution simulation (S4), introducing anthropogenic disturbance for the last 11,000 years of the simulation, shows increase of the soil loss rate for the last 11000 years of the model from 0.68 cm/kyr (Base Simulation) to a rate of 1.05 cm/kyr. The Agricultural revolution simulation ends with an average soil depth of 14.5 cm.

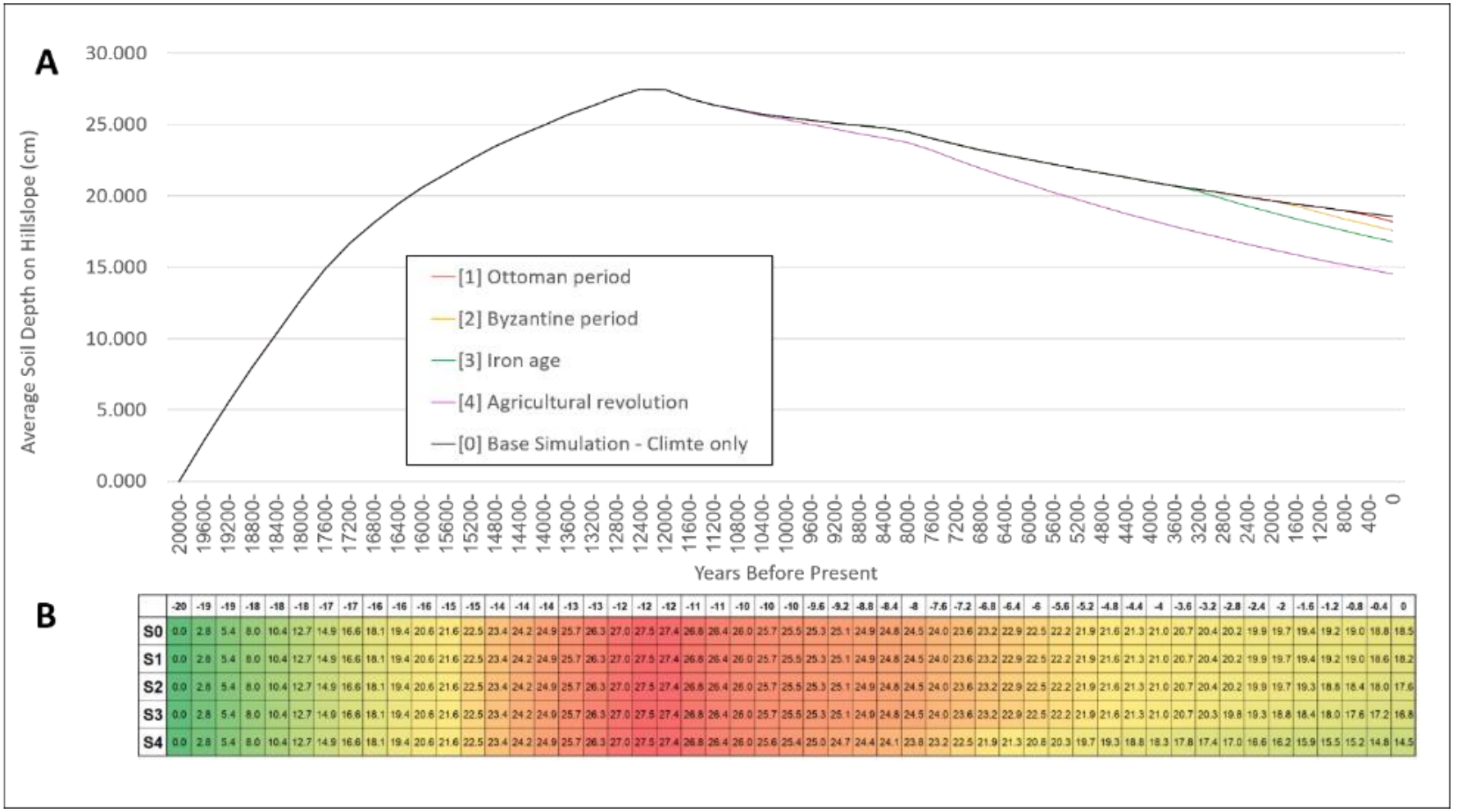

	-20	-19	-19	-18	-18	-18	-17	-17	-16	-16	-16	-15	-15	-14	-14	-14	-13	-13	-12	-12	-12	-11	-11	-10	-10	-10	-9.6	-9.2	-8.8	-8.4	-8	-7.6	-7.2	-6.8	-6.4	-6	-5.6	-5.2	-4.8	-4.4	-4	-3.6	-3.2	-2.8	-2.4	-2	-1.6	-1.2	-0.8	-0.4	0
S0	0.0	2.8	5.4	8.0	10.4	12.7	14.9	16.6	18.1	19.4	20.6	21.6	22.5	23.4	24.2	24.9	25.7	26.3	27.0	27.5	27.4	26.8	26.4	26.0	25.7	25.5	25.3	25.1	24.9	24.8	24.5	24.0	23.6	23.2	22.9	22.5	22.2	21.9	21.6	21.3	21.0	20.7	20.4	20.2	19.9	19.7	19.4	19.2	19.0	18.8	18.5
S1	0.0	2.8	5.4	8.0	10.4	12.7	14.9	16.6	18.1	19.4	20.6	21.6	22.5	23.4	24.2	24.9	25.7	26.3	27.0	27.5	27.4	26.8	26.4	26.0	25.7	25.5	25.3	25.1	24.9	24.8	24.5	24.0	23.6	23.2	22.9	22.5	22.2	21.9	21.6	21.3	21.0	20.7	20.4	20.2	19.9	19.7	19.4	19.2	19.0	18.6	18.2
S2	0.0	2.8	5.4	8.0	10.4	12.7	14.9	16.6	18.1	19.4	20.6	21.6	22.5	23.4	24.2	24.9	25.7	26.3	27.0	27.5	27.4	26.8	26.4	26.0	25.7	25.5	25.3	25.1	24.9	24.8	24.5	24.0	23.6	23.2	22.9	22.5	22.2	21.9	21.6	21.3	21.0	20.7	20.4	20.2	19.9	19.7	19.3	18.8	18.4	18.0	17.6
S3	0.0	2.8	5.4	8.0	10.4	12.7	14.9	16.6	18.1	19.4	20.6	21.6	22.5	23.4	24.2	24.9	25.7	26.3	27.0	27.5	27.4	26.8	26.4	26.0	25.7	25.5	25.3	25.1	24.9	24.8	24.5	24.0	23.6	23.2	22.9	22.5	22.2	21.9	21.6	21.3	21.0	20.7	20.3	19.8	19.3	18.8	18.4	18.0	17.6	17.2	16.8
S4	0.0	2.8	5.4	8.0	10.4	12.7	14.9	16.6	18.1	19.4	20.6	21.6	22.5	23.4	24.2	24.9	25.7	26.3	27.0	27.5	27.4	26.8	26.4	26.0	25.6	25.4	25.0	24.7	24.4	24.1	23.8	23.2	22.5	21.9	21.3	20.8	20.3	19.7	19.3	18.8	18.3	17.8	17.4	17.0	16.6	16.2	15.9	15.5	15.2	14.8	14.5

Figure 10: A – average soil depth for all the simulations over time of the simulation. All of the simulation overlaps until -8400 BC. The blue line represents the base simulation, pink line - simulation [4], green line – simulation [3], yellow line – simulation [2], red line – simulation [1]. B – a table of the absolute value of the soil depth for each time step for each simulation.

The trends described above are witnessed again when examining the spatial absolute values of the soil depth along the simulations (Figure 11). The baseline simulation (S0), as all the other simulations, starts with a shallow (0.5 cm), spatially uniform, soil veneer. Soil accumulation, erosion and deposition started shaping the soilscape soon after. Up to -12000 BP all the simulations are equivalate, thus Figure 11 does not show these years. As the simulation proceeds, the soil is eroded and more of the hillslope becomes soil depleted (soil thickness of 0 cm), representing exposed bedrock. For all the simulations there are more outcrops at the higher area of the hillslope with close to uniform soil distribution along the simulations. The erosion intensifies as a function of the time human activity is introduced in each scenario. A direct outcome of the intensified erosion is more outcrops as the human interference is longer, e.g. at the end of S4 there are more outcrops than S3. Although the amount of outcrops is visible, the differences in the soil depth are negligible. It is assumed that the differences in the period of human interference causes a different distributions of similar soil amounts.

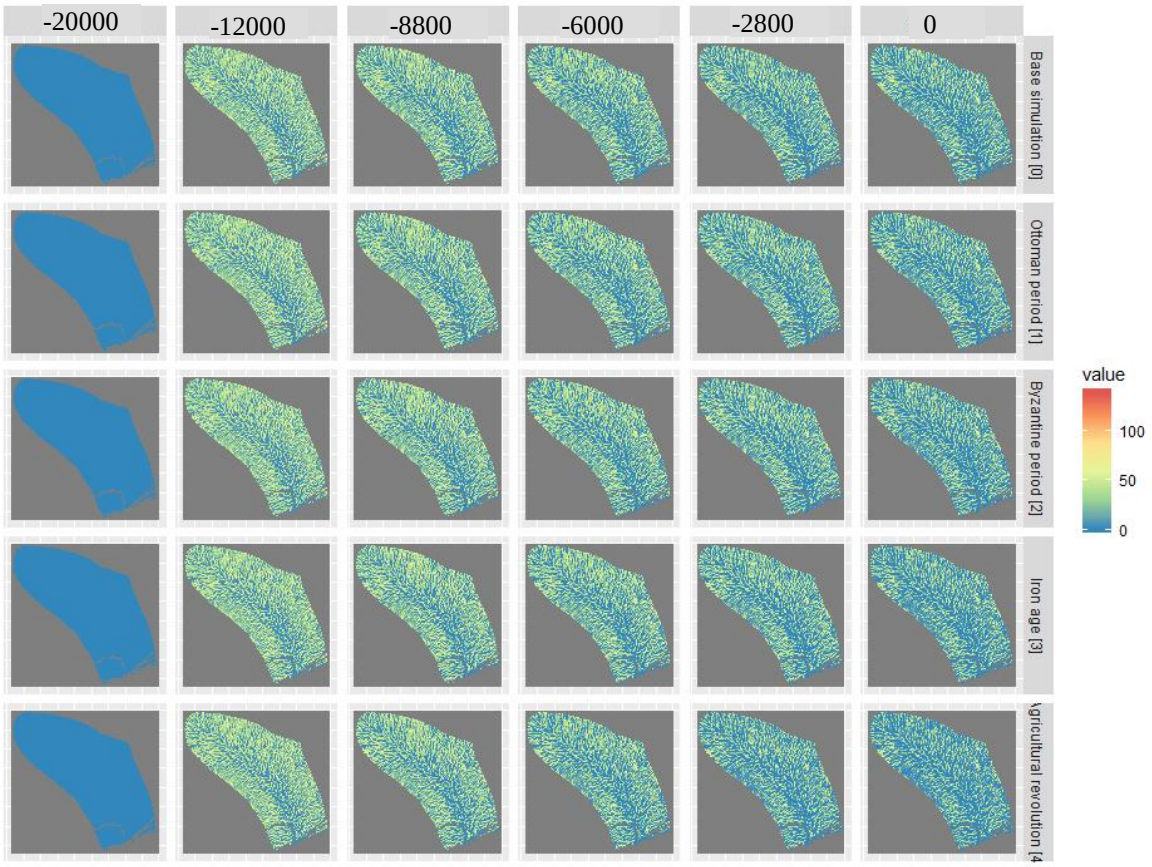

Figure 11: Soil depth (cm) on the study site hillslope. X axis - Time line (BP), Y axis - Simulation name.

If comparing the final soil depth (2000 BC) of the base simulation (S0) to the one of the longest human influence on the soil (S4), there are significantly more patches of exposed bedrock at the end of the S4 simulation (Figure 12). Most of the soil loss took place in the lower areas of the hillslope. There are a few isolated locations on the hillslope where soil depth is higher at the S4 simulation, mainly along the center of the hillslope, represented by warm colors in Figure 12.

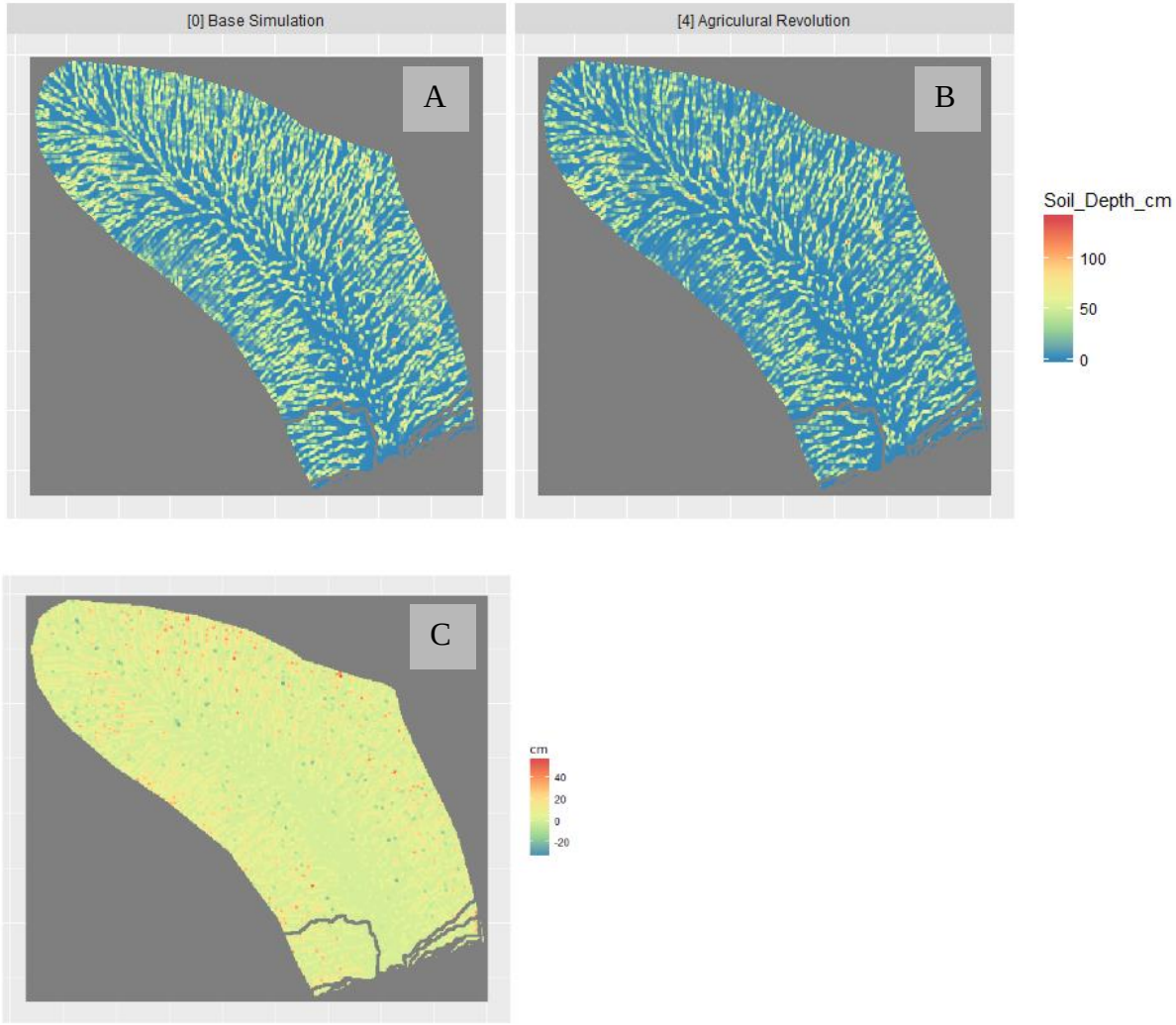

Figure 12: A – Soil depth (cm) at the end of the Base Simulation [0]. B - Soil depth (cm) at the end of the Agricultural Revolution Simulation [4]. C – Difference raster (A-B=C).

3.3. Particle size distribution

For the baseline Simulation (S0), as for all the simulations up to -9000 BC, the d50 (median particle size at the surface layer in each cell) are relatively fine (silt size - around 0.0105 mm), which is indicative of the dominance of Aeolian deposition on soil production in the simulations. The particles at the lower areas are coarser and are around 0.012 mm. These areas are also characterized by having patches of smaller particles (under 0.010 mm) between them (Figure 13). This description is identical for all simulations d50 outputs until -12,000 BP (after 8,000 model years). For -12,000 BP most of the d50 on the hillslope is silt or sand grain size, this is the first iteration with pebbles larger than 2 mm. From -12,000 BP

the amount of pebbles increases and stabilizes on a similar distribution until the end of the simulation.

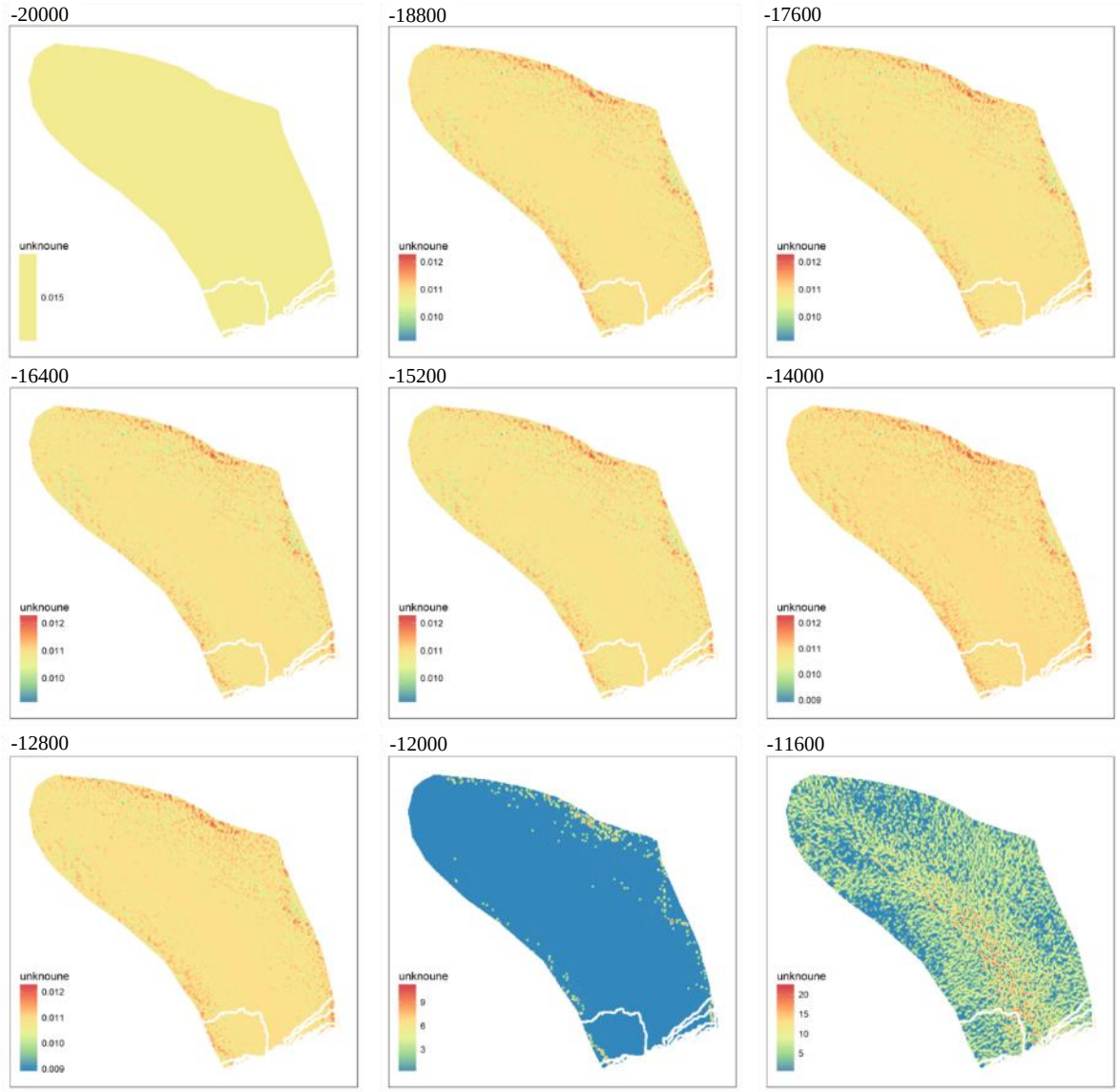

Figure 13: Median particle size (mm) for the surface layer in the Base Simulation [0]

Introduction of human activity considerably altered PSD in all human influenced simulations (S1-S4) (Figure 14). Generally, there is a coarsening trend following human influence was introduced, resulting in a distribution of finer particles at the lower section and coarser particles at the upper sections of the hillslope. Although the change in particle size is significant immediately after the introduction of the human influence, the later outputs maintain a similar distribution and what appears such a transformation between one steady state to another. This can be attributed to the increase in the simulated discharge increase in

response to human disturbance, allowing for courser particles to be entrained by overland flow. After these relatively coarse particles have been transported downslope, the surface PSD remains relatively unchanged.

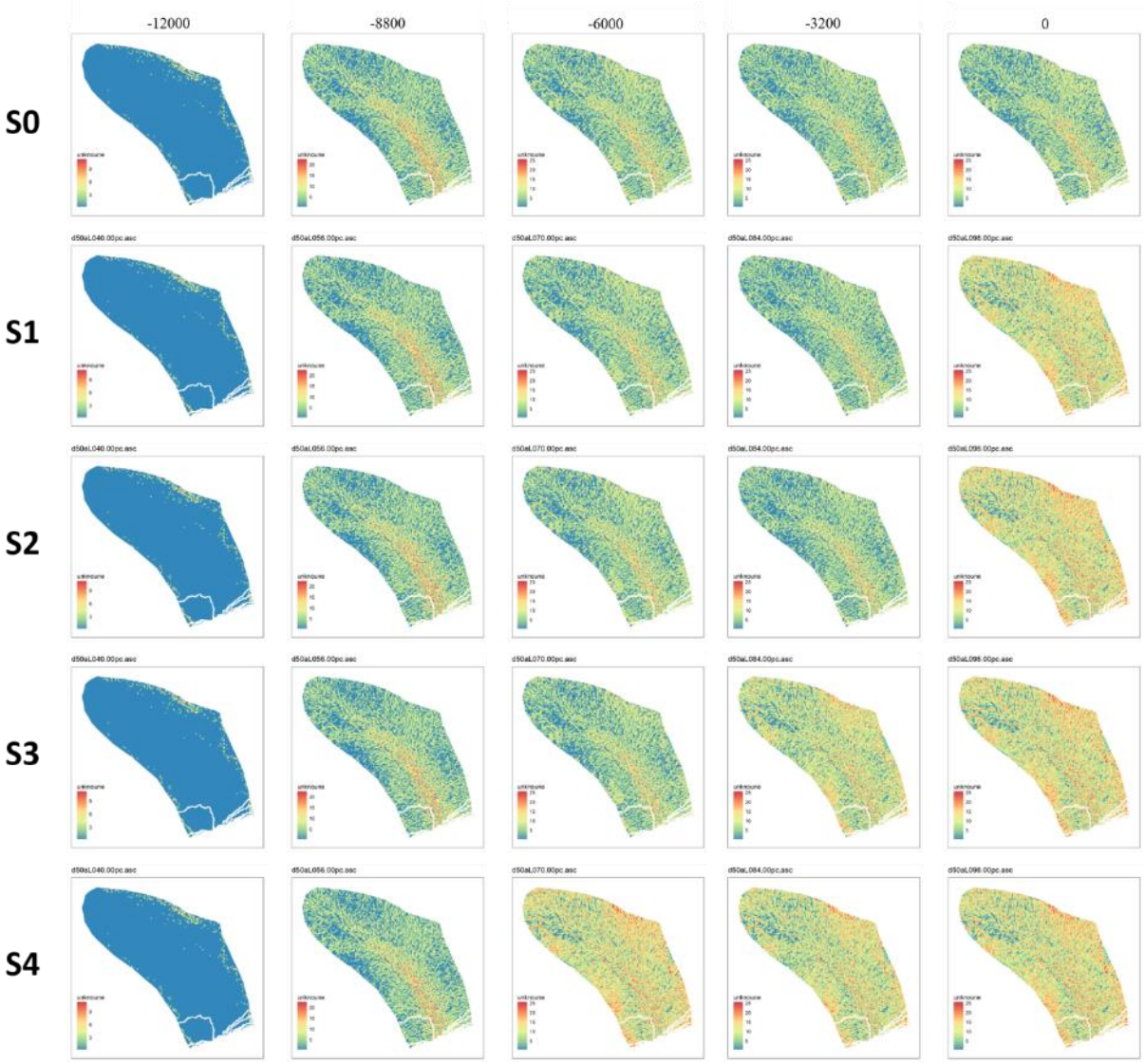

Figure 14: Median Particle size on the surface layer for all the simulations from the beginning (left) to the end (right) of the simulation.

4. Discussion

The mARM5D model was mainly used, in previous studies, to conduct conceptual studies using synthetic data (e.g. Cohen et al., 2015). In this study, we applied the model on a new field site for which we had limited field data. As part of this project, new measurements were conducted of high-resolution PSD analysis from 43 pits on the hillslope, soil depth from 43 pits, and a high-resolution DEM acquired from an airborne LIDAR sensor with a 0.5m spatial resolution that was down scaled to 1m resolution. Despite existing literature on rates of soil creep, aeolian deposition, discharge and soil erodibility, there were no such measurements from or near the study site. An extensive sensibility analysis and calibration process was conducted in order to estimate the most appropriate calibration parameter values. That procedure included more than 1,000 model simulations that contained pre-defined parameter space, based on the relevant literature. Despite of the extensive calibration and sensibility analysis, this study should still be considered as a semi-synthetic research that can expand the current knowledge on soilscape evolution response to varying degree of anthropogenic disturbance, but not a fully realistic predictor of the site's soilscape history. The aim of this research was, therefore, to advance out understanding about the region's potential soilscape response to varying degrees (duration) of human disturbances.

Soil distribution corresponded quite well with observed distribution, characterized by sections of exposed bedrock, entwined with pockets of soil (Figure 1A). The range of average soil depth resulting from the extensive sensitivity analysis was 1.8-34.1cm. This means that even for the most "favorable" parameter values, within the parameter space chose in this analysis, the resulting soil thickness is quite low and corresponds well to the modern (observed) soilscape. This suggests that it is unlikely that the site ever had a considerably deep layer of soil (more than 1m), given the assumed soil production rate (based on literature) and pre-human erosion rates (based on the sensitivity analysis). Most of the evidence of major human–induced soil degradation are from sites that contained deep soils.

In those sites human activities changed the soilscape equilibrium, exposing well developed soils to erosion. This does not seem to be the case in this site.

Based on the evidence of sharp changes in vegetation cover in northern and central Israel (Baruch, 1986; Neumann et al., 2010), combined with what is known on the rich history of human settlements in the study site area (Dagan, 1992, 2002, 2006; Me'ir, 2012; Uziel and Maeir, 2005), we can assume that deforestation took place in the study site region as well. If this was the case, we can't blame anthropogenic activity in destroying this landscape and introducing mass soil erosion to the region.

Anselmetti et al. (2007) quantified the influence of the ancient Maya culture on soil erosion rates, caused by deforestation. They show how even a small and traditional population can introduce major influence on erosion rates. Their study was based on soil cores recovered from Lake Salpetén, that is the sink of a closed drainage basin, in the tropical lowlands of northern Guatemala. When combining the data, they concluded that the Maya culture in this area is responsible to an average amount of 80 cm of soil loss over the entire catchment, with higher and lower rates throughout the catchment.

It is known as well, that deforestation took place in Northern and central Israel. Baruch (1994) shows how the differences in the local flora driven from the sea of Galilei imply on a massive deforestation undergone 3000 years BP. Neumann et al.(2010) found evidence of deforestation and profound vegetation changes in central Israel dated to begin 3500 years ago, by studying sediment cores and outcrops from the Dead-Sea.

The calibrated model was used to run five climatic and anthropogenic scenarios. The maximum difference in site-averaged soil depth was 22% between the baseline scenario (S0 – no human activity) and the scenario that simulated the longest human activity (S4 - beginning of the agricultural revolution). This is followed by differences of 9%, 5% and 2% for the rest of the other scenarios (S1-S3), which simulated shorter human activities. While a 22% difference between the two extreme simulations is considerable, in absolute values it translates to only 4 cm. This is because there is no significantly deep soil accumulation on

the hillslope prior to the introduction of human influence in the simulations. The soil depth maps show that longer anthropogenic influence resulted in more bedrock outcrops, although not in a wide scale. This is manly caused by the increased rates of fluvial sediment transport during the simulated anthropogenic influence period. It is likely to assume that the small difference in average soil depth between the simulations is due to the mechanisms that distribute the similar amount of soil in different patterns along the hillslope. When comparing the final results of the model for the extreme simulations (S0 and S4) (Figure 12a and b) the differences are emphasized. There are distinguishly more bedrock outcrops (blue color represents 0 cm of soil) in S4, and it seems as if the similar amount of soil is accumulated in deeper soil pockets down the hillslope, therefore exposing more bedrock outcrops upslope. The difference raster (Figure 12C) reinforces this by simply showing grid cells of high difference and low difference (in cm) between the two simulation results. It is clear from the image that most of the difference take place at the lower areas of the hillslopes, likely due to the higher fluvial erosion rates in the S4 simulation. Stronger fluvial erosion means that soil particles which were not entrained by fluvial soil movement in simulation S0 have been entrained by fluvial transport in S4 due to increase in discharge and soil erodibility, accumulating greater amount of soil at the lower areas of the hillslopes.

In contrary to soil thickness, particle size distribution (PSD) at the surface layer (upper 0.5 cm) of the hillslope, reveals a strong response to anthropogenic activity. Whereas soil thickness is slightly affected from anthropogenic activities, PSD undergoes a rapid change to a coarser distribution. This is an outcome of two main processes: (1) greater transport capacity due to greater simulated Q in S4, and (2) anthropogenic activities that increase surface erosivity. From the soil thickness point of view, anthropogenic activity accelerates soil erosion that was already occurring due to climate fluctuation starting 12 kyr BP (Figure 10). From the PSD point of view, climate fluctuation changes the steady-state PSD 12 kyr BP, leading to particle coarsening. After anthropogenic activity is introduced an additional change from one steady-state to another is apparent. This can be explained by changes in

parameter values, simulating human activity (increase in discharge and erodibility), allow for particles that were not available for entrainment in the pre-human period to be entrained and transported downslope. This led to high erosion rates, transforming the PSD and soil distribution from one steady-state to another.

Avni et al. (2006) concluded that in the Negev region (arid climate) of Israel (south of the study site), climate fluctuation was responsible for changes in soil properties, rather than anthropogenic factors. In this study anthropogenic factors were found to have some influenced the soil depth and PSD in the Shfela region, yet not as drastic as in studies from southern Europe (van Andel et al., 1990), Central America (Anselmetti et al., 2007) or the Loess Plateau in China (Zheng, 2006).

5. Conclusions

The extensive sensitivity analysis process provided an in depth understanding of the model parameter relationship. For this site, when no climate fluctuation is simulated, the dominant soil transport mechanism is the diffusive mechanism. This is changed when introducing climate fluctuation and human interference by increasing the discharge and erodibility. The parameters chosen for the simulation scenarios were efficient taking consideration that there are no rate data on the site.

The results of the simulation scenarios analysis suggest that it is unlikely that the site ever had a considerably deep layer of soil (more than 1m). Therefore, it is hard to connect anthropogenic activity as the main factor leading to the soil-depleted hillslopes observed in the Shfela region of Israel. It demonstrates that climate fluctuation, leading to lower aeolian deposition and higher soil erosion rates, could have shifted local soil evolution from a net accumulation mode (or static equilibrium), mainly based on aeolian deposition, to soil erosion mode, driven by increase in discharge and diffusive mechanisms.

While this study does not offer a conclusive answer to the question 'was the Shfela region of Israel underwent extensive human influence, leading to a soil depleted landscape?' it does shed light on the trends of soil thickness and PSD over the past 20 kyr. Based on the model's outputs, a strong relationship is found between the PSD on the surface layer to the introduction of human interference. This is demonstrated by the immediate shift from one steady state to a different one just after introducing human interference to the model. The PSD trend is shifted to a coarser surface of the hillslope. primarily on the main mechanisms that may have drove the soil to its present condition.

This research advances our understanding on the soil-human interaction, by connecting the enhanced discharge and erodibility to thinner soils with more outcrops. The research raises important questions about the use of models in the field of soilscape evolution, due to the amount of assumptions that need to be made and the extensive data required to run them in a high-resolution scale. Further sensitivity analysis and calibration processes should take place in different climate zones and human history in order to strengthen the robustness of the models and methodology. Mechanisms of Bioturbation and hydrology are recommended to be added in future versions of the model as these will add a remarkable contribution when simulating soil-scape evolutions in wetter climates.

It would be fruitful to pursue further research about the historical soil thickness and PSD at the higher boundary of the semi-humid region in order to achieve a wider picture of the anthropogenic influence on soil properties through history at different locations.

6. References

Ackermann O et al. 2014. Palaeoenvironment and anthropogenic activity in the southeastern Mediterranean since the mid-Holocene: The case of Tell es-Safi/Gath, Israel. Quaternary International **328**–**329**: 226–243.DOI: 10.1016/j.quaint.2014.02.016

van Andel TH, Zangger E, Demitrack A. 1990. Land Use and Soil Erosion in Prehistoric and Historical Greece. Journal of Field Archaeology **17**: 379–396.DOI: 10.1179/009346990791548628

Anselmetti FS, Hodell DA, Ariztequi D, Brenner M, Rosenmeier MF. 2007. Quantification of soil erosion rates related to ancient Maya deforestation. Geology **35**: 915–918.DOI: 10.1130/G23834A.1

Avni Y, Porat N, Plakht J, Avni G. 2006. Geomorphic changes leading to natural desertification versus anthropogenic land conservation in an arid environment, the Negev Highlands, Israel. Geomorphology **82**: 177–200.DOI: 10.1016/j.geomorph.2006.05.002

Baruch U. 1986. The Late Holocene Vegetational History of Lake Kinneret (Sea of Galilee), Israel. Paléorient **12**: 37–48.DOI: 10.3406/paleo.1986.4407

Baruch U. 1994. Palynological Evidence for Human Impact upon the Flora of the Land of Israel in Antiquity. Qadmoniot: A Jurnal for the Antiquities of Eretz-Israel and Bible Lands : 47–63.

Bowman D, Karnieli A, Issar A, Bruins HJ. 1986. Residual Colluvio-aeolian Aprons in the Negev Highlands (Israel) as a Paleo-Climatic Indicator, Palaeogeogr. Palaeogeography, Palaeoclimatology, Palaeoecology **56**: 89–101.

Bruckner H. 1986. Man's Impact on the Evolution of the Physical Environment in the Mediterranean Region in Historical Times. GeoJournal **13**: 7–17.

Bruins HJ, Yaalon DH. 1992. Parallel advance of slopes in aeolian loess deposits of the northen Negev, Israel. Israel Journal of Earth Sciences **41**: 183–199.

Butzer KW. 2005. Environmental history in the Mediterranean world: cross-disciplinary investigation of cause-and-effect for degradation and soil erosion. Journal of Archaeological Science **32**: 1773–1800.DOI: 10.1016/j.jas.2005.06.001

Cohen S, Svoray T, Sela S, Hancock G, Willgoose G. 2017. Soilscape evolution of aeolian-dominated hillslopes during the Holocene : investigation of sediment transport mechanisms and climatic-anthropogenic drivers. Earth Surface Dynamics : 1–24. DOI: 10.5194/esurf-5-101-2017

Cohen S, Willgoose G, Hancock G. 2009. The mARM spatially distributed soil evolution model: A computationally efficient modeling framework and analysis of hillslope soil surface organization. Journal of Geophysical Research: Solid Earth **114**: 1–15.DOI: 10.1029/2008JF001214

Cohen S, Willgoose G, Hancock G. 2010. The mARM3D spatially distributed soil evolution model: Three-dimensional model framework and analysis of hillslope and landform responses. Journal of Geophysical Research: Earth Surface **115**: 1–16.DOI:

10.1029/2009JF001536

Cohen S, Willgoose G, Svoray T, Hancock G, Sela S. 2015. The effects of sediment transport, weathering, and aeolian mechanisms on soil evolution. Journal of Geophysical Research: Earth Surface **120**: 260–274.DOI: 10.1002/2014JF003186.Received

Dagan Y. 1992. Archaeological Survey of Israel: Map of Lakhish . Jerusalem

Dagan Y. 2002. Survey of Tel Zafit region. Excavations and Surveys in Israel 114.83 **114**: 83:e85.

Dagan Y. 2006. Archaeological Survey of Israel, Map of Amazya (109) . Jerusalem

Dan J, Koyumdjisky H, Yaalon DH. 1962. Principles of a proposed classification for the soils of Israel. 410–421 pp.

Dan J, Yaalon DH. 1966. Trends in soil development with time in the Mediterranean environments of Israel. 137–145 pp.

Dan J, Yaalon DH, Koyumdjisky H, Raz Z. 1972. The Soil Association Map of Israel. Israel Journal of Earth-Science **21**: 29–49.

Dietrich WE, Perron JT. 2006. The search for a topographic signature of life. Nature **439**: 411–418.DOI: 10.1038/nature04452

Garcia-Ruiz JM. 2010. The effects of land uses on soil erosion in Spain: A review. Catena **81**: 1–11.DOI: 10.1016/j.catena.2010.01.001

Goodfriend GA. 1987. Chronostratigraphic studies of sediments in the Negev desert, using amino acid epimerization analysis of land snail shells. Quaternary Research **28**: 374–392.DOI: 10.1016/0033-5894(87)90005-6

Inbar M. 1992. Rates of fluvial erosion in basins with a Mediterranean type climate. CATENA **19**: 393–409.DOI: 10.1016/0341-8162(92)90011-Y

Israel Meteorological Service. 2011. Israel climate atlas [online] Available from: http://www.ims.gov.il

Israel Science and Technology Directory. 2018. Israel Science and Technology Directory [online] Available from: www.science.co.il

Jenny H. 1941. Factors of soil formation. A system of quantitative pedology . Dover Publications: New York

Kaplan JO, Krumhardt KM, Zimmermann N. 2009. The prehistoric and preindustrial deforestation of Europe. Quaternary Science Reviews **28**: 3016–3034.DOI: 10.1016/j.quascirev.2009.09.028

Meʾir A. 2012. Tell es-Safi/Gath I: the 1996-2005 seasons . Harrassowitz Verlag: Wiesbaden

Minasny B, Finke P, Stockmann U, Vanwalleghem T, McBratney AB. 2015. Resolving the integral connection between pedogenesis and landscape evolution. Earth-Science Reviews **150**: 102–120.DOI: 10.1016/j.earscirev.2015.07.004

Mohammad AG, Adam MA. 2010. The impact of vegetative cover type on runoff and soil erosion under different land uses. Catena **81**: 97–103.DOI: 10.1016/j.catena.2010.01.008

Neumann FH, Kagan EJ, Leroy SAG, Baruch U. 2010. Vegetation history and climate fluctuations on a transect along the Dead Sea west shore and their impact on past societies over the last 3500 years. Journal of Arid Environments **74**: 756–764.DOI: 10.1016/j.jaridenv.2009.04.015

Picard L, Golani Y, Bentor Y k, Vroman A, ZAK. 1965. Geological map of Israel 1:250,000

Recep E ,Balikesir U, Abdullah S, Balikesir U. 2015. Impacts of anthropogenic factors on land degradation during the anthropocene in Turkey. Journal of Environmental Biology **36**: 51–58.

Singer A. 2007. The Soils of Israel . Springer Science & Bbusiness Media: Berlin

Sneh A. 2008. Geological map of Israel 1:50,000

Tarboron DG (Utah SUL. 1997. A new method for the determination of flow directions and upslope areas in grid digital elevation models. Water Resources Research **33**: 309–319.

Tarboton DG. 2010. Terrain Analysis Using Digital Elevation Mod- els (TauDEM) [online] Available from: http://hydrology.neng.usu.edu/taudem

Temme AJAM, Vanwalleghem T. 2016. LORICA – A new model for linking landscape and soil profile evolution: Development and sensitivity analysis. Computers & Geosciences **90**: 131–143.DOI: 10.1016/j.cageo.2015.08.004

Uziel J, Maeir AM. 2005. Scratching the Surface at Gath: Implications of the Tell es-Safi/Gath Surface Survey. Tel Aviv **32**: 50–75.DOI: 10.1179/tav.2005.2005.1.50

Vaks A, Bar-Matthews M, Ayalon A, Matthews A, Frumkin A, Dayan U, Halicz L, Almogi-Labin A, Schilman B. 2006. Paleoclimate and location of the border between Mediterranean climate region and the Saharo–Arabian Desert as revealed by speleothems from the northern Negev Desert, Israel

Vanwalleghem T, Stockmann U, Minasny B, McBratney AB. 2013. A quantitative model for integrating landscape evolution and soil formation. Journal of Geophysical Research: Earth Surface **118**: 331–347.DOI: 10.1029/2011JF002296

Villamil MB, Amiotti NM, Peinemann N. 2001. Soil Degradation Related To Overgrazing in the Semi-Arid Southern Caldenal Area of Argentina. Soil Science **166**: 441–452.DOI: 10.1097/00010694-200107000-00002

Wieder M, Sharabani M, Singer A. 1993. Phases of calcrete (Nari) development as indicated by micromorphology. Developments in Soil Science **22**: 37–49.DOI: 10.1016/S0166-2481(08)70396-9

Willgoose GR, Sharmeen S. 2006. A One-dimensional model for simulating armouring and erosion on hillslopes: 1. Model development and event-scale dynamics. Earth Surface Processes and Landforms **31**: 970–991.DOI: 10.1002/esp.1398

Yaalon DH. 1997. Soils in the Mediterranean region: what makes them different?

CATENA **28**: 157–169.DOI: 10.1016/S0341-8162(96)00035-5

Zheng F-L. 2006. Effect of Vegetation Changes on Soil Erosion on the Loess Plateau. Pedosphere **16**: 420–427.DOI: 10.1016/S1002-0160(06)60071-4

Zilberman E. 1992. The Late Pleistocene sequence of the northwestern Negev flood plains - A key to reconstructing the paleoclimate of southern Israel in the last glacial. Israel Journal of Earth Sciences **41**: 155–167.

Zohary D, Hopf M, Weiss E. 2012. The origin and spread of domesticated plants in Southwest Asia, Europe, and the Mediterranean Basin . Oxford University Press on Demand